

Characterizing and predicting the self-folding behavior of weft knit fabrics.

Chelsea Amanatides¹, Oana Ghita², Ken E Evans², Genevieve Dion^{1,3}

1. Center for Functional Fabrics, Drexel University, USA
2. College of Engineering, Mathematics and Physical Sciences, University of Exeter, UK
3. Antoinette Westphal College of Media Arts and Design, Drexel University, USA

Abstract

Self-folding behavior is an exciting property of weft knit fabrics that can be created using just front and back stitches. This behavior is easy to create, but not easy to anticipate and currently cannot be predicted by existing computer aided design (CAD) software that controls the CNC knitting machines. This work identifies the edge deformation behaviors that lead to self-folding in weft knits, and methods to characterize the mechanical forces driving these behaviors with regard to chosen manufacturing parameters. With this data and analysis of the fabric deformations, the self-folding behavior was purposely controlled using calculated scaling factors. Furthermore, theoretical equations were developed to mathematically predict these scaling factors, minimizing the trial and error required to design with self-folding behavior and create textiles with novel engineered properties. By understanding the mechanisms responsible for creating these three-dimensional self-folding textiles, they can then be designed in a programmable manner for use in technical applications.

1. Introduction

Using qualitative and quantitative analysis, this work aims to understand and predict self-folding in weft-knit fabrics, an exciting behavior with potential for use in advanced manufacturing textile systems. While self-folding can be engineered into a variety of systems, from polymer assemblies to shape memory alloys, in weft knit textiles this structure driven behavior is inherent. Self-folding occurs naturally, due to the chosen stitch pattern. Folded textile structures can be created that show promise for use in deployable architecture, space exploration, defense and more, similar to the work that has been explored for origami structures.¹⁻³ Unlike origami folded structures, *no post-processing procedures are required to produce these structures*. In addition the folds produced by knitting are both less constrained topologically and not damaged by the folding process itself. If better understood, this self-folding property of weft knit textiles could be exploited for the development of novel engineered textiles with new and exciting properties⁴, such as auxetic behavior,⁵⁻¹¹ increased sound absorption⁸, and impact resistance.^{12,13}

1.1 The weft knit structure

Weft knitting is a method of textile production that creates a fabric from series of intermeshing loops of yarn. The geometry of the knit loop is shown in Figure 1a. When assembled in a fabric, these loops are referred to as stitches. In the weft knit structure, horizontal rows of stitches are referred to as courses and the vertical columns of stitches are referred to as wales.

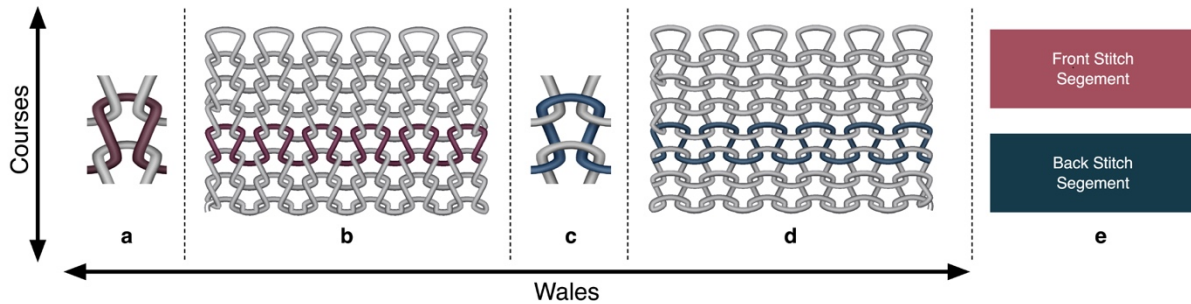


Figure 1. Front stitches and back stitches, simulations of a) the front stitch, b) jersey knit made from all front stitches, c) the back stitch, and d) jersey knit made from all back stitches, e) representative colors to indicate segments of front stitches and back stitches

A knit textile made from all the same stitches is known as a jersey knit. This can be produced using a single bed knitting machine. Figure 1 (a and b) shows front stitch knitting, which can be distinguished by the small “v” shapes visible, formed by the vertical legs of the stitches. Figure 1 (c and d) shows back stitch knitting, which is distinguishable by the small curves visible, formed by the horizontal head and tails of the stitch. Front and back knit stitches are structurally symmetric, however the side from which they are viewed determines their nomenclature in the knit structure. Using a two-bed weft knitting machine, *self-folding fabrics* can be produced that incorporate both front stitches and back stitches on the same continuous side of the fabric. Stitch patterns presented in this study use pink to represent front stitches and the color blue to represent back stitches. Handknitting terminology may refer to these stitches as knit and purl respectively.

1.2 Complex Self-Folding Structures

Yarn relaxation is a behavior that occurs after the knitting process, both by hand and by machine. As the yarn is pulled through to form each stitch, tension is applied on the yarn. As soon as the fabric leaves the needles this tension is released and the yarn starts to relax, producing the self-folding effect. Additionally, the three-dimensional shape of a knitted loop has been well documented and contributes to the presence of self-folding deformation behaviors. When switching between a front stitch and a back stitch, either along the course direction or wale direction, the yarn is moved into a second plane, bridging the gap between the front and back

needle beds (or in the case of hand knitting, moving between the front and back of the needle). Figure 1. demonstrates the topology of a front to back stitch transition in both course and wale directions, as represented on a helicoid-based modeling system presented by Knittel et al. and Waedekar et al. In Figure 1a, it can be seen how the yarn traverses between the front and back bed, as front and back stitches are created side by side, along the wale direction. Once removed from the tension of the needles, the yarn that spans between the beds will relax and a curling effect will pull the front and back stitches closer together, producing two distinct surfaces in the finished fabric. Considering a transition from front to back stitch that occurs along the course direction, it can be seen from Figure 1b how the loop is required to deform to span the distance between the beds. Once removed from tension, these loops begin to relax, again producing a curling effect at the interface.

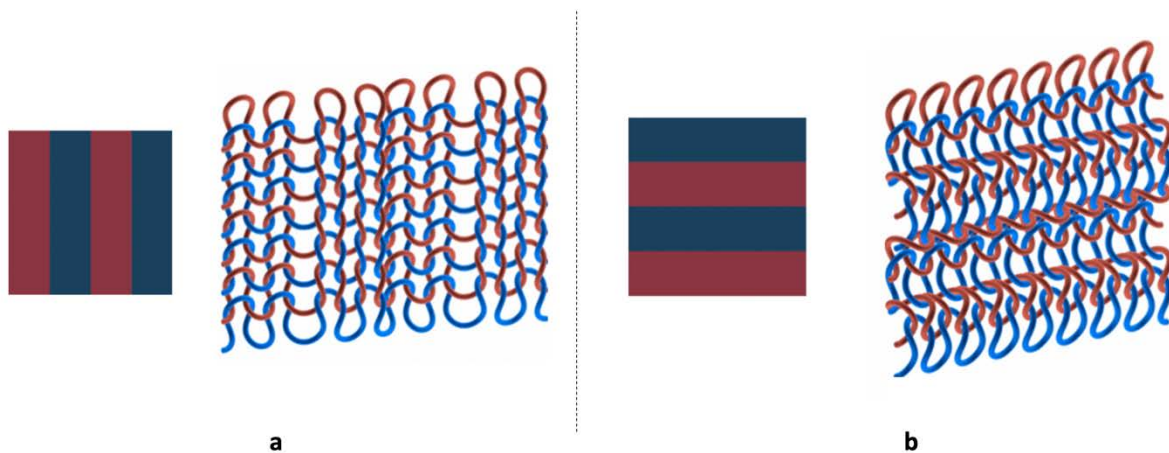


Figure 1. Front and back stitches represented on helicoid modeling system, demonstrating the three-dimensionality of stitches.

The rib knit structure is a self-folding structure which provides stretch and dimensionality. Therefore, it is often found at the cuffs and hems of sweaters (Figure 2a). It is easily produced using a simple repeating pattern of columns of front stitches and back stitches. Using the same two stitches organized into different geometric patterns, wide varieties of self-folding fabric structures can be formed (Figure 2b-d)). All these structures are created as a result of yarn relaxation and the 3-dimensionality of knitted loops.

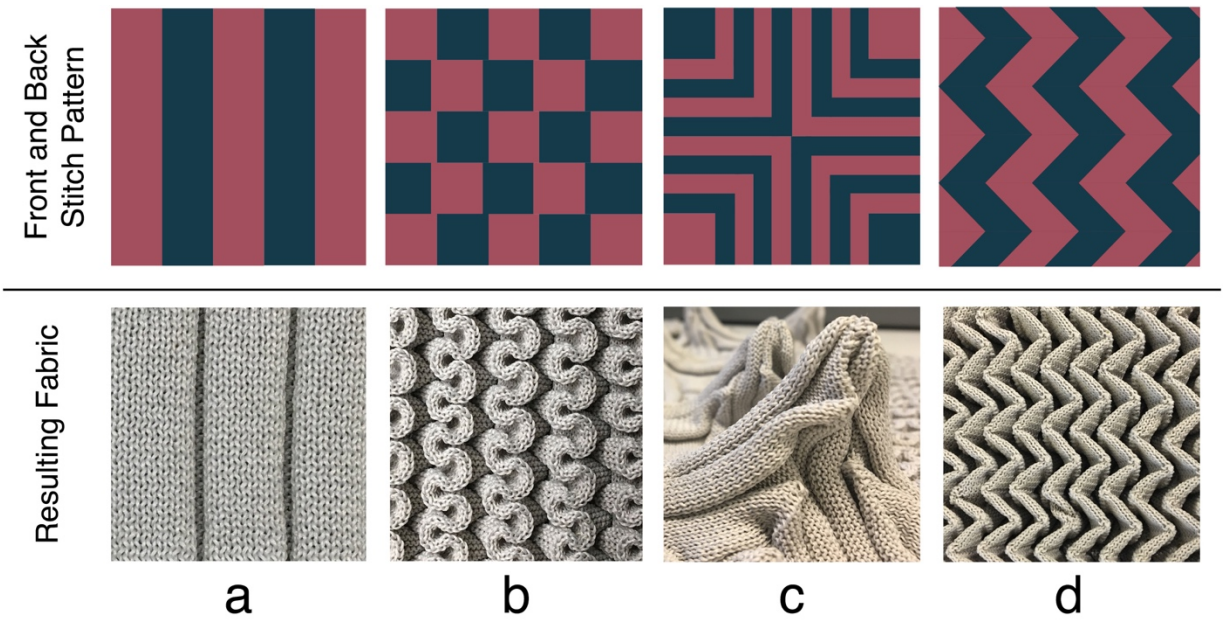


Figure 2. Examples of self-folding structures made from front and back stitch patterns.

1.3 Modeling of weft knit structures

Self-folding behavior is relatively simple to produce using combinations of front stitches and back stitches. The challenge, however, lies in understanding *where and how* the folds will occur, to control the specific type of structure that results as the textile relaxes and deforms. At present, industry standard textile modeling software cannot predict self-folding behavior in knits. Figure 3 shows the current modelling capability of Shima Seiki SDS-One APEX knit design software¹⁴. Consequently, design of these structures has been largely dependent on trial and error.

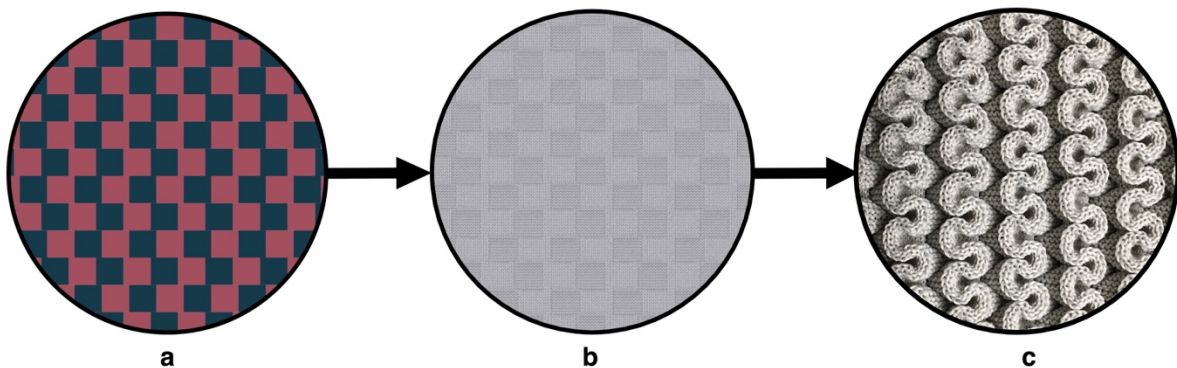


Figure 3. Programming and modeling of self-folding behavior, a) a front and back stitch pattern, b) the corresponding simulation produced in Shima Seiki SDS One Apex Software⁴³ representing the real fabric held in tension, and c) the resulting fabric after yarn relaxation.

In literature, many approaches have been utilized to model the behavior of textiles, including weft knit textiles. These tend to fall within the categories of geometric¹⁵⁻²³ and mechanical models,²⁴⁻³⁰ graphics models³¹⁻³⁷, computer aided design tools,³⁸⁻⁴¹ and parametrized models.⁴²⁻⁴⁴ Recently, work has been published by researchers at Carnegie Mellon University, describing systems that have been developed to ease the steep learning curve required for designing and programming for textile machinery such as weft knitting machines.³⁸⁻⁴¹ This work allows the use of three dimensional meshes, typically used in other computer aided design systems, for the development of knitting machine instructions. All of these bodies of work help to translate textile production to a modern manufacturing platform. However, none of these available systems currently demonstrate prediction of the self-folding behavior in knits.

This study sought to understand and predict self-folding knit structures without the need to model the individual stitches. This was achieved by considering the macro-scale components composed of segments of front stitches or back stitches, and how these components interact with one another. We then identified how to measure the mechanical behaviors of these components *and* analyze how they interact, working toward a predictive system. This approach facilitates faster prediction and tuning of the fabric behavior as compared to complex stitch modeling, which require geometric and physics-based modeling of the individual stitch structures, as well as yarns. In addition, the resulting models are far less computing-intensive than those requiring modelling at the resolution of individual stitches.

2. Analysis of Self-Folding Behaviors

2.1 Materials

All samples in this study were made from 100% mercerized extra fine merino wool (9037 Supra Merino, 7,500ypp, 3.5 twists per centimeter, S-twist. Silk City Fibers, Paterson, NJ, USA), on a Shima Seiki SWG041N 15-gauge industrial knitting machine, using the same conditions for tensioning of the yarn.

2.2 Qualitative Analysis: Boundary condition behaviors

To begin to understand the self-folding behavior of weft knit structures made using front stitches and back stitches, a jersey knit fabric was analyzed. The jersey knit was produced from all front stitches. The same fabric could be produced by alternatively using all back stitches. In all jersey knit fabrics, regardless of yarn material, characteristic behavior occurs. The top and bottom edges of front stitch segments will naturally roll forwards, while the side edges will naturally roll backwards. The top and bottom edges of back stitch segments will naturally roll backwards, while the side edges will naturally roll forwards. Figure 4 depicts a jersey knit sample with an equal number of courses and wales, demonstrating this characteristic edge deformation behavior.

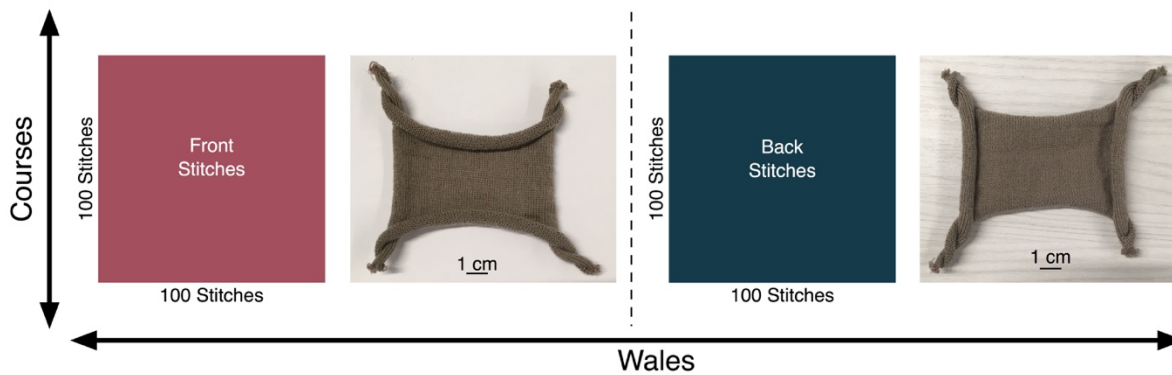


Figure 4. Characteristic edge rolling behavior of jersey knit fabric, as seen from a) the front stitch side, and b) the back stitch side.

This effect is magnified when considering fabric samples in which the number of courses far exceeds the number of wales, or vice-versa, as shown in Figure 5. When the number of wales is much smaller than the number of courses, the rolling effect on the side edges overtakes the rolling effect on the top and bottom edges, and the entire structure rolls into a scroll shape towards the back stitch side. In the opposite case, the opposite effect is observed in which a scroll shape is formed, consisting of the back stitch side rolling completely towards the front stitch side, as shown in the right side of Figure 5.

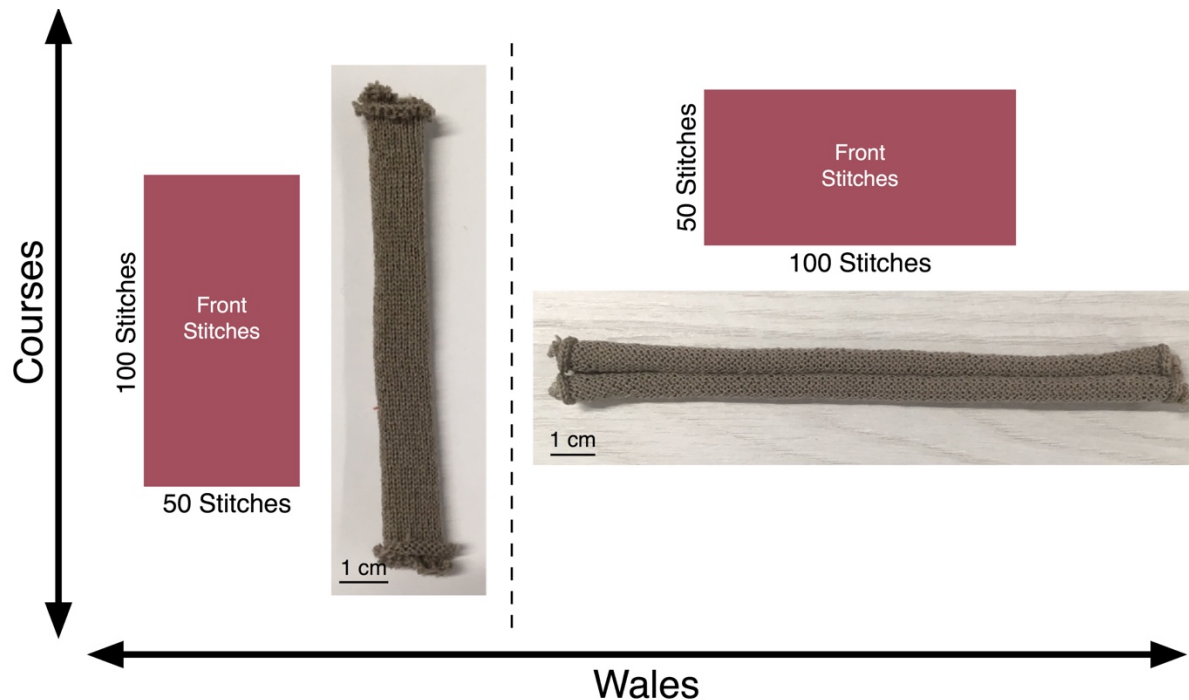


Figure 5. Jersey knit fabric samples, with isolated course or wale direction rolling behavior.

2.3 Qualitative Analysis: Combined edge effects

When combining fields of front and back stitch segments as shown in Figure 6, it can be observed that out of plain deformation is formed as a result of the competing edge rolling behavior of each segment. The fields can be combined sequentially as the courses are knit (one row occurring after the other during knitting), creating a *horizontal transition* between front stitches and back stitches, or fields can be placed side by side, changing from one wale to another, creating a *vertical transition* between the fields of front stitches and back stitches. Figure 6 demonstrates the resulting fabric that occurs from these two basic combinations of front and back stitches. The type of transition between front and back stitches determines the direction in which the fabric will fold, based on the boundary condition behavior of the individual segments. In the case of the horizontal transition, the top edge of the back stitch segment rolls over the front stitch segment at the border. In the case of the vertical transition, the front stitch segment rolls over the back stitch segment at the border. Since a weft knit structure consists of a grid of courses and wales of stitches, it follows that on the individual stitch level, *any complex self-folding pattern can be broken down into these horizontal or vertical transitions between front stitches and back stitches*. Understanding the deformation behavior of these simple patterns serves as a building block for prediction of behavior in more complex stitch patterns.

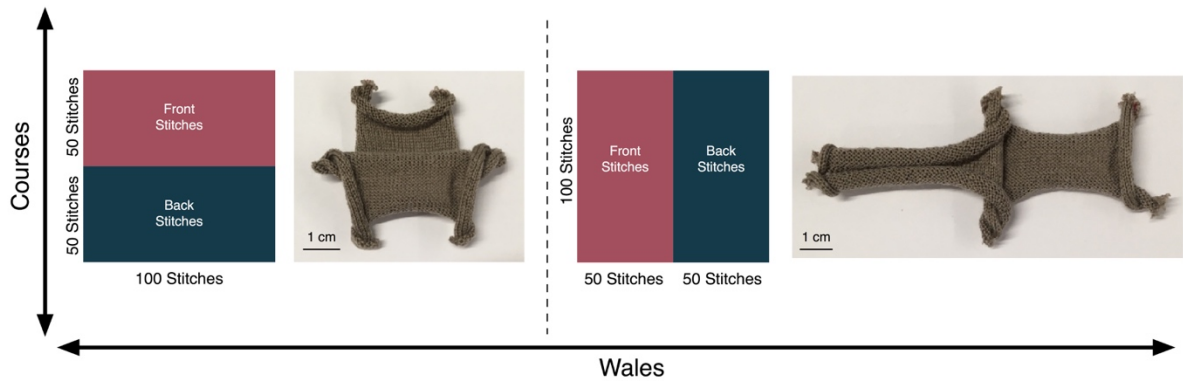


Figure 6. Self-folding behavior resulting from competition of edge rolling behavior.

2.4 Quantitative Analysis: Mechanical Testing Methods

Four types of knit samples were produced for mechanical characterization to develop a method to transition from qualitative to *quantitative* evaluation of these boundary condition behaviors. The stitch patterns of these samples are shown in Table 1, showing the locations of the grip portions of the fabric that were held between the two plates of the metal grips during testing. Jersey samples were made to be approximately 25mm in width and height (not including the grip portion of the fabric). Horizontal and vertical transition samples were made to be approximately 25mm in width and height *when completely unfolded* (not including the grip portion of the fabric).

Table 1. Front and back stitch patterns for mechanical characterization testing samples.

Sample Code	J1	J2	H	V
Description	Jersey Sample	Jersey Sample	Horizontal Transition Sample	Vertical Transition Sample
Stitch Pattern				
Representative Sample				

To produce these samples, the stitch dimensions required to produce samples of 25mm in height and width at varying stitch values were calculated using Equations (1) and (2). A reference sample (R) was produced, and its measurements (course (C_R) and wale (W_R)) were used to calculate the dimensions of the new sample (N) with the desired.

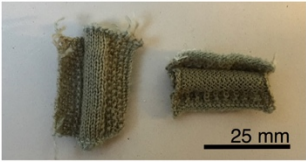
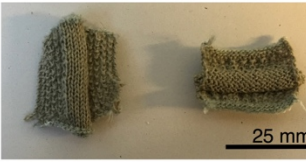
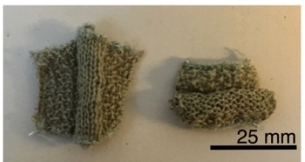
$$W_N = \frac{(W_R)w_N}{w_R} \quad (1)$$

$$\text{and } C_N = \frac{(C_R)h_N}{h_R} \quad (2)$$

Where, w_R is the measured width of the number of wales in the reference sample, h_R is the measured height of the number of courses in the reference sample, and W_N , and C_N , are the *required* number wales and courses, to achieve the desired sample width and height (w_N and h_N). These calculations are required because the aspect ratio of a stitch is rarely 1:1, so to achieve a sample of equal width and height, different amounts of courses and wales will likely be needed. Plain jersey samples (sample types J1 and J2, Table 1) were characterized to provide a comparison of jersey extension behavior to that of the self-folding samples. These stitch patterns were then split horizontally or vertically into one field of front stitches and one field of back stitches, creating two different folding samples that were proportionally equivalent (sample types H and V, Table 1).

Samples were produced at three different stitch values, 22, 28 and 40 to assess the effects of changes in manufacturing parameters on the self-folding behavior. This stitch value determines the amount by which the needle pulls down on a stitch during the knitting process, and thus the stitch density of the resulting fabric. The measured fabric gauges for swatches made at *stitch values 22, 28 and 40* are depicted in Table 2, along with representative horizontal and vertical transition samples shown to scale. In order to maintain consistent *physical* dimensions between all three stitch values, the *stitch* dimensions differ between the three sets. While these stitch values are specific to Shima Seiki machines, and may result in different fabric densities based on yarn selection, these stitch value numbers are used within this manuscript as a convenient way to reference and differentiate between the samples that were tested.

Table 2. Horizontal and vertical folding samples with corresponding gauge measurements.

Shima Seiki Stitch Value	22	28	40
Courses per cm	13.3	9.8	7.7
Wales per cm	8.5	7.6	5.3
Horizontal and Vertical Transition Samples	Vertical Transition Horizontal Transition 	Vertical Transition Horizontal Transition 	Vertical Transition Horizontal Transition 

All samples were tested at least 24 hours after fabrication. Fabric samples were affixed to a card and placed into the grips of an Instron tabletop testing machine with a 5 Newton load cell. The sample card sides were cut before the test began, and each sample was “pre-stretched” by extending to the full unfolded length, then returning to the initial gauge length. All tests were then carried out at a rate of 25 mm/min. Force and extension data was recorded. Jersey samples (J1 and J2) began tests in their relaxed, flat state, and were extended to 150% of their original relaxed length. Transition samples (H and V) began tests in their fully relaxed, *folded* state, and were extended to an end gauge length of 25mm. This ensured that the transition samples were pulled just to the point of being completely unfolded. Therefore, the *final* gauge length of the transition samples was approximately the same as the *initial* gauge length of the jersey samples. Engineering strain was calculated and graphed against “stitch force,” the force recorded by the load frame,

divided by the number of stitches in the width or height of the sample (perpendicular to the direction of extension). Graphed data for these sample were averaged from sample sets of 9 specimens of each type.

3. Results

3.1 Quantitative Analysis: Mechanical Characterization Data

Figure 7 presents the stitch force plots for extension of jersey sample types J1 and J2 at the three different stitch values, average from three samples each. Looking at the stitch structure, anisotropic properties can be assumed and are observed during mechanical characterization. As the fabric is pulled so that the spacing between each wale increases (J2), the stitches are pulled open before the load is distributed to the yarn. As the fabric is pulled so that the spacing between each course increases (J1), the force is distributed more immediately to the fibers of the yarns.

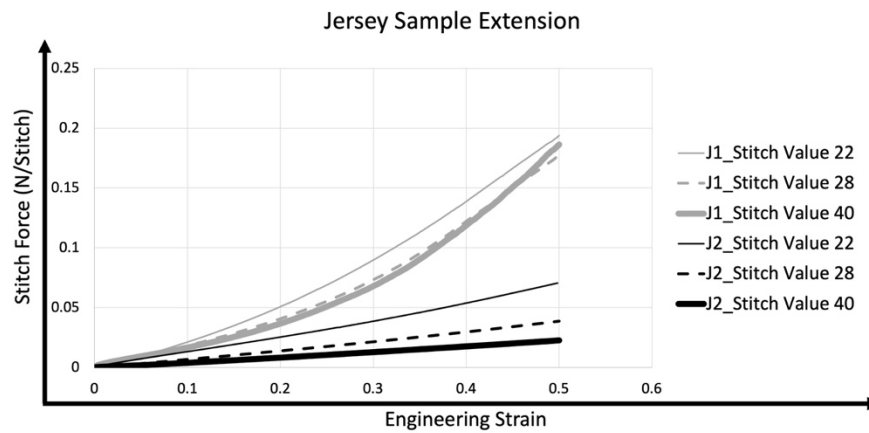


Figure 7. Averaged J1 and J2 extension at varying stitch values.

Figures 8, 9 and 10 present the stitch force plots for horizontal and vertical transition folding sample types at the three different stitch values, calculated using the collected load-extension data. The range of standard deviation along the curve is shown. The normalized data demonstrates that on average, the horizontal transitions are stronger than the vertical transitions, regardless of the stitch value used. Plots with all sample curves are available in the Supplemental Data section (a-c). Figure 11 compares the datasets for horizontal and vertical transition folding sample at three different stitch values.

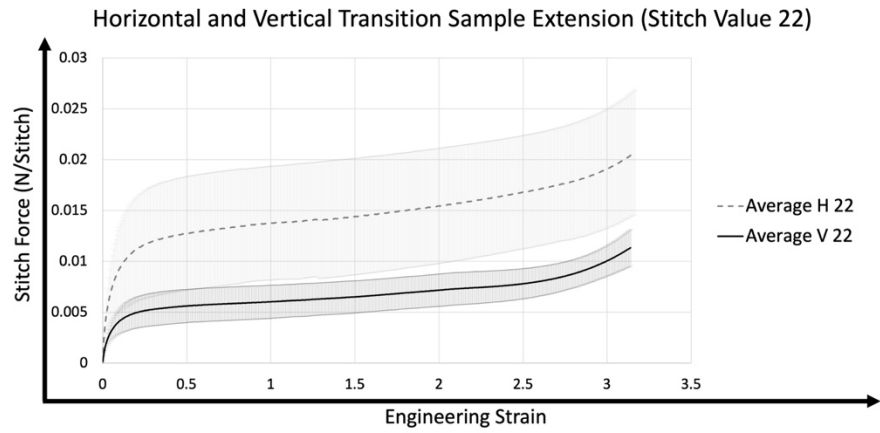


Figure 8. Characterization of horizontal and vertical folding samples made at stitch value 22.

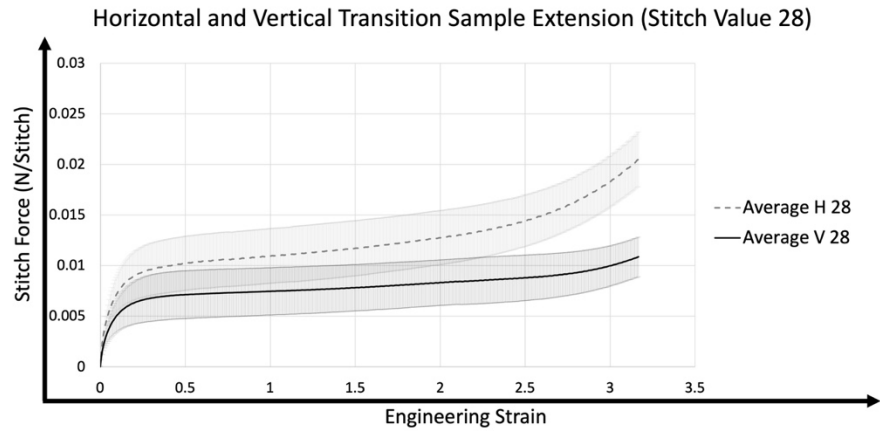


Figure 9. Characterization of horizontal and vertical folding samples made at stitch value 28.

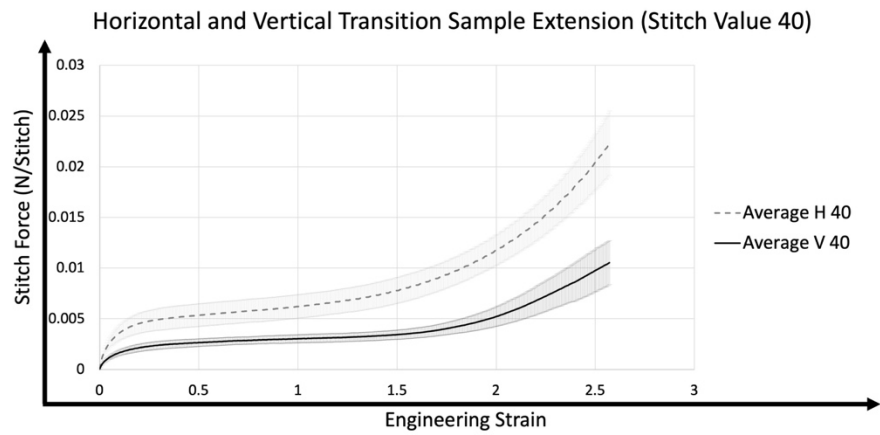


Figure 10. Characterization of horizontal and vertical folding samples made at stitch value 40.

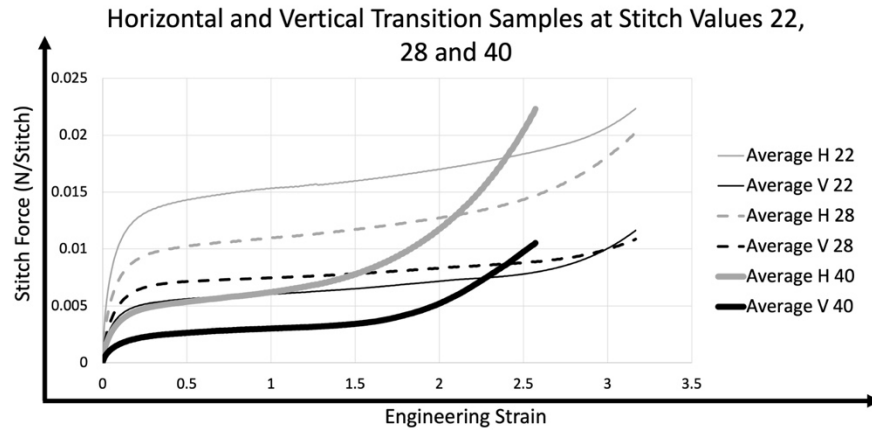


Figure 11. Comparison of all horizontal and vertical folding transitions

Considering the generalized shape of the curves recorded for the horizontal and vertical folding samples, three regions of behavior were identified as shown in Figure 12. The shape of these curves are comparable to those measured for elastomeric materials, which present three distinct regions of behavior; a) initial stiff response, b) strain induced softening, and c) strain induced hardening.⁴⁵ For the three regions measured here, they can be described more specifically as follows; (a) *Region I* is the region where the unfolding begins. A certain threshold of force must be reached before *Region II* can begin; (b) *Region II* can be considered the ‘stable unrolling region’. In this region, the samples exhibit a linear behavior; (c) *Region III* is the region in which the sample approaches the completely unfolded state. Physically the behavior begins to transition into that of a plain jersey fabric. As the sample is completely unfolded, the applied force begins to pull on the stitches themselves, rather than the fold. Therefore, similarities can be observed between the shape of this region of the curve and the shape of the stitch force curve for the jersey samples in Figure 7. An interesting analogy can be made between knit fabrics and elastomeric materials; the properties of the knit are a combination of the properties of the fibers, of the yarn made from the fibers and of the geometry of the knit, while the properties of the elastomer is a combination of the physical properties of the individual macromolecules, and the geometry in terms of entanglements, knots, and crosslinks.

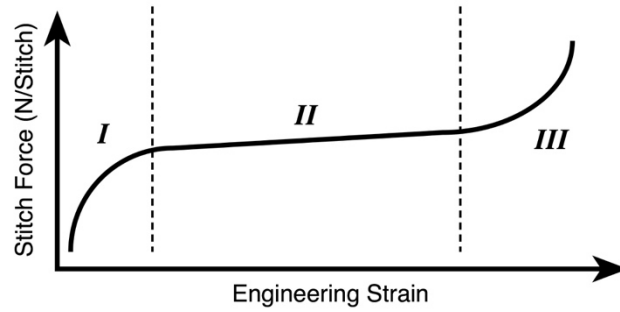


Figure 12. Generalized stitch force curve for folding samples, Region I) threshold unrolling force, Region II) stable unrolling, Region III) transition into jersey behavior

In addition to the general trends, in *region I* the force thresholds vary both with orientation of the front stitch to back stitch transition (horizontal vs. vertical folds) as well as stitch value, as shown in Table 3. The longest linear segment (in *region II*) was identified by drawing tangent lines along the edges of the curve until the longest continuous section was identified, and the slope of this segment was used to determine the stitch modulus. Threshold force was determined as the beginning point of this linear region.

Table 3. Region I Average Threshold Force and Region II Average Stitch Moduli for Transition Samples

Orientation of Front Stitch to Back Stitch Transition	Stitch Value	Threshold Force (mN/stitch)	Region II Stitch Modulus (mN/Stitch)
Horizontal	22	15.3 +/- 5.4	1.5 +/- 0.2
Horizontal	28	9.8 +/- 2.9	1.6 +/- 0.6
Horizontal	40	5.4 +/- 0.8	1.9 +/- 0.4
Vertical	22	5.4 +/- 1.7	0.9 +/- 0.1
Vertical	28	7.3 +/- 3.6	0.6 +/- 0.3
Vertical	40	2.6 +/- 0.5	0.8 +/- 0.1

* For samples made at stitch value 22; values shown in Table 2 were calculated from a set of 8 specimens, due to the inability to identify a linear *region II* segment in the data collected from one of the specimens.

The trend in the horizontal transition samples is logical with regards to friction effects, in the denser samples (made using a lower stitch value), yarns are held more tightly together, making it harder for stitches to move and shift past one another as the sample unfolds. In the vertical transition samples, it is still observed that samples made at stitch value 40 (the least dense) exhibit the weakest folding forces. Samples made at stitch value 22 and 28 however, do not follow the same trend, and the measured forces are closer to one another than in the horizontal transition samples. Considering the physical meaning of stitch value, *the amount by which the needle pulls down on the stitch*, this could be explained by the fact that stitch value more *directly* affects the

stitch length and only *indirectly* affects the stitch width. The measured gauges of the fabric reflect this, showing a greater change in height of the stitch, than width of the stitch between samples made at stitch value 22 and 28. Since the vertical transition samples change from front stitch to back stitch across the width of the fabric, the resulting change in the border conditions is less than in the horizontal transition, where the change from front stitch to back stitch occurs across the length of the fabric. The change in dimensions of the stitch value 40 samples on the other hand, are significant enough in both height and width, to exhibit the weakest folding forces in both sample types.

Observing the *region II* moduli in Table 3, the values for all horizontal transition samples are of similar magnitude regardless of stitch value used. Similarly, the modulus for all vertical transition samples are of similar magnitude, regardless of stitch value used. This trend suggests that once deformation has begun, the force driving the behavior in this region are more dependent on the type of fold (i.e., the specific stitch pattern/structure) than on the stitch value.

3.2 Combining Qualitative Observations and Quantitative Data to Control the Self-folding Behavior

To map the folding pattern effects, the developed understanding of boundary condition edge deformations was used to analyze a stitch pattern and identify the directionality of folding between segments of front stitches and back stitches. Next, the measured threshold force ratios were incorporated. This allowed for improved prediction of folding by understanding where horizontal transition folding overpowers vertical transition and *vice-versa*. Figure 13 demonstrates the application of the mechanical characterization results to a front and back stitch pattern, showing how a specific behavior that occurs can, firstly, be predicted and then, by changing the force ratios, be purposely changed.

Starting with a programmed checkerboard pattern of front and back stitch segments where each square has equal amounts of stitches in the width and height, i.e. 20x20 stitches, (Figure 13A), the fabric produced shows only the back stitches on the face of the fabric, pushing all of the front stitch segments underneath. However, in some cases, design specifications may require a fabric with the same type of folding, that instead equally balances the contributions of horizontal and vertical folds. To achieve this, the front and back stitch program can be scaled by the measured fabric gauge, using Equations (1) and (2) described in Section 2.3 to produce segments of front and back stitch stitches that are the same *physical* height and width dimensions (Figure 13B). This produces a fabric where the back stitches remain dominant, and the front stitches, though more visible, are still pushed below the surface. If the program is then scaled further, by the measured ratio of threshold forces (horizontal/vertical) (Figure 13C), a fabric can be produced that equally balances the contributions of horizontal and vertical folds. Both front and back stitch segments are present on the surface of the fabric, and the overall fabric shape is no longer skewed diagonally.

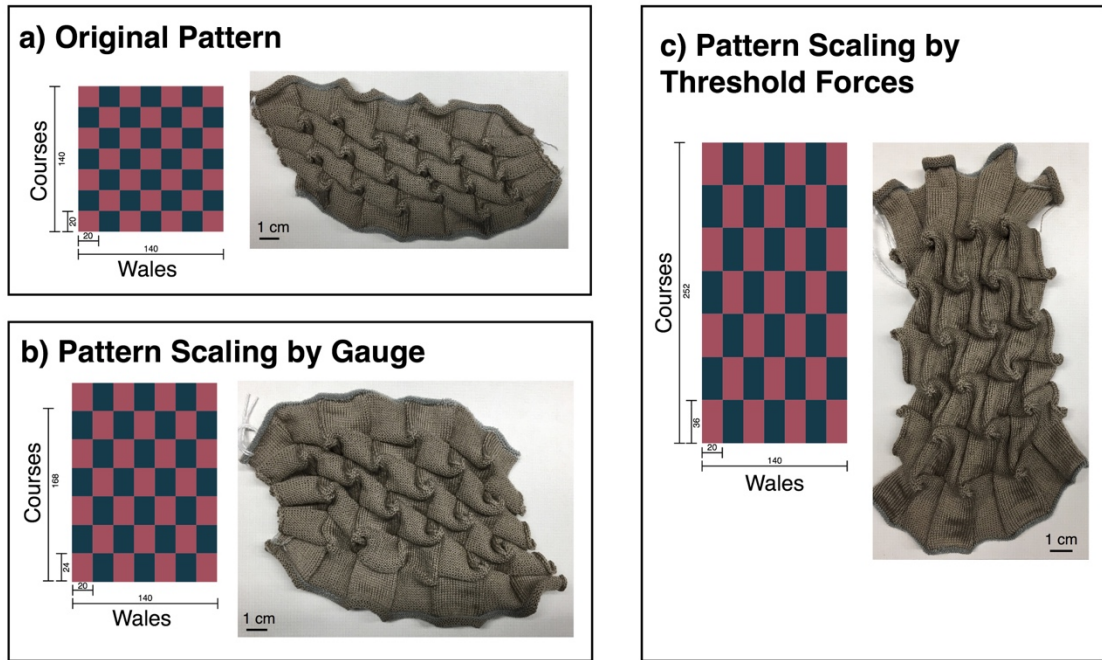


Figure 13. Controlling the self-folding behavior in the weft knit structure; a) original stitch pattern, b) stitch pattern scaled using stitch gauge, c) stitch pattern scaled using threshold forces.

3.3 Theoretical Equations

While the experimentally determined scaling-ratio is useful in creating a specific self-folding behavior, it is unrealistic to fabricate test samples and carry out the mechanical characterization tests each time a fabrication parameter is changed. Therefore, an equation was developed to theoretically predict the stitch force curves and therefore the scaling factor, of fabrics made at varying stitch values, circumventing the need to repeat the characterization experiment for each. Instead, characterization of folding samples could be carried out at a single “reference stitch value” which is then used to theoretically calculate the behavior at other stitch values, only requiring the knowledge of courses per cm and wales per cm at the other stitch values. These equations were developed first for horizontal front-to-back stitch transition samples, then for vertical front-to-back stitch transition samples.

3.3.1 Predicting the Horizontal Transition Extension Behavior

Using the experimental data collected for the horizontal transition folding samples made at stitch values 22, 28 and 40, the following equation was determined.

$$\text{Stitch force } (H_N) = \left(\frac{B}{A}\right)H_R \quad (3)$$

$$\text{where } A = \frac{N}{R} \quad (4)$$

$$\text{and } B = \frac{hw_N}{hw_R} \quad (5)$$

where H_N is the theoretically determined stitch force curve for samples made at the new stitch value N . H_R is the best fit equation for the experimentally determined stitch force curve determined from a set of samples made at reference stitch value R . (This equation was determined using was identified using the “trendline” data fitting function of Microsoft Excel.) hw_N is the number of wales in a 25mm width for the new stitch value, and hw_R is the number of wales in a 25mm width for the reference stitch value. Equation (3) utilizes both the input stitch value (from equation (4)) and the measured stitch dimensions (from equation (5)). This reflects the fact stitch dimensions can change with a change in yarn, tension or other variables, even when the stitch value remains the same.

Each stitch value was tested as a reference value to use to predict the stitch force curves of the samples made at the remaining two stitch values (Figure 14). The predicted curves agree with the experimental curves in *Region I*, and the beginning of *Region II*, providing predicted threshold forces. The predicted curves do not match for *Region III*, however only the threshold force was necessary to determine the scaling ratio that was used to control the self-folding behavior. Further work will be conducted in the future to explore development of robust equations capable of predicting the entire data curve.

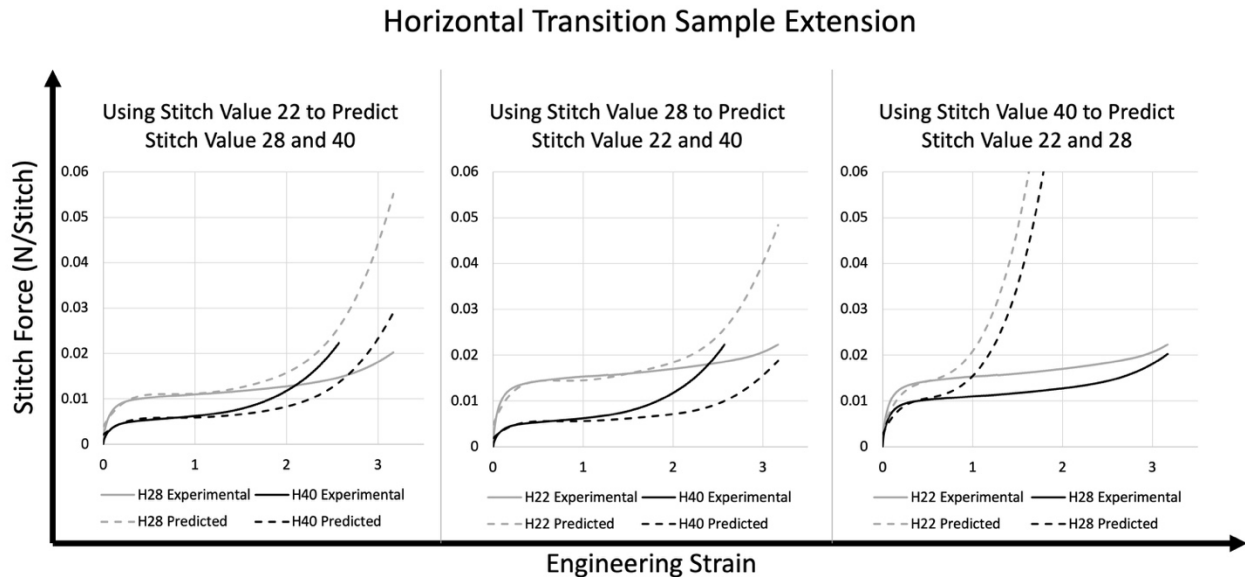


Figure 14. Theoretical prediction of stitch force curves in horizontal transition samples

Equation 3 was then used to predict the curve that should result if the horizontal transition samples were produced at a stitch value of 34. In this case, 28 was used as the reference stitch value. Afterwards, samples were fabricated at this new stitch value of 34 and the mechanical characterization tests were repeated, showing agreement between the theoretical and experimental results (Figure 15).

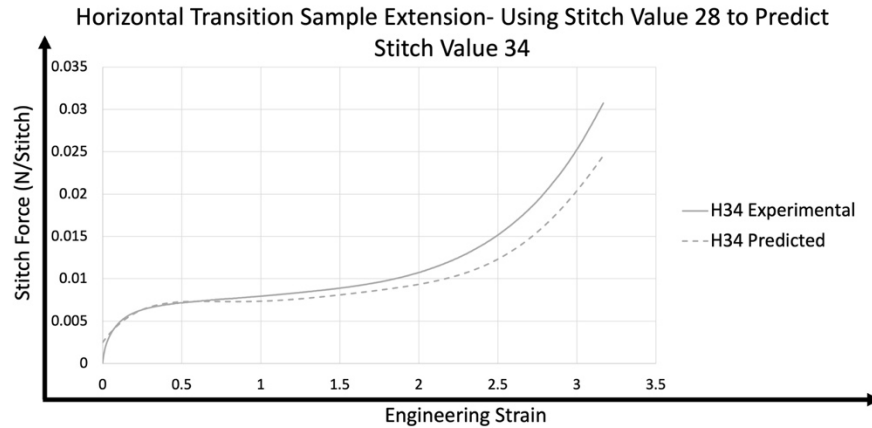


Figure 15. Predicting the stitch force curve of a horizontal transition sample made at stitch value 34.

3.3.2. Predicting the Vertical Transition Extension Behavior

First it was noted that the vertical transition samples made at stitch value 22 did not follow the same trend as all other samples (where an increase in stitch value resulted in a decrease in folding strength) (Figure 11 - Average Vertical Transition). To eliminate experimental error as a source of this result, a second sample set for horizontal and vertical transition folding samples made at stitch value 22 were fabricated and tested. The same results were observed. Considering the higher stitch density of these samples it was hypothesized that past a certain threshold, stitches are no longer able to move and slide as easily past their neighboring stitches, therefore affecting the deformation mechanisms, and requiring additional variables in the predictive equation. Therefore, at this time, vertical transition samples were produced at stitch value 34, to provide an additional data set for testing. The experimental results of stitch value 34 vertical transition samples are compared to the results at stitch values 28 and 40 in Figure 16

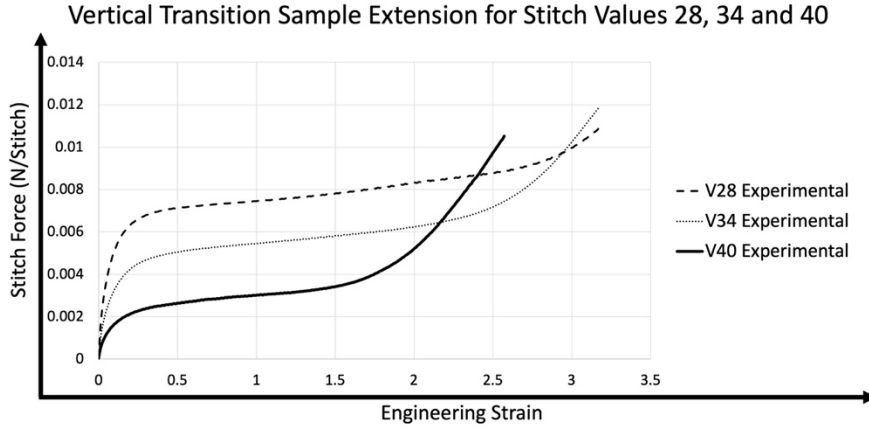


Figure 16. Comparing the stitch force curves of vertical transition samples made at stitch values 22,28, and 40.

Next, Equation 3 was applied similarly to the vertical transition samples, however this did not produce theoretical curves that matched the experimental data. It was therefore, hypothesized that the vertical transition sample exhibited nonlinear behavior. The following equation was determined that could be used to predict the vertical transition behaviors,

$$\text{Stitch force } (V_N) = V_R \left(\frac{B}{C} \right)^p \quad (6)$$

$$\text{where, } C = \frac{R}{N} \quad (7)$$

$$\text{and } B = \frac{v_{CN}}{v_{CR}} \quad (8)$$

and $p=10.5$, where V_N is the theoretically determined stitch force curve for samples made at the new stitch value N , and V_R is the best fit equation for the experimentally determined stitch force curve determined from a set of samples made at reference stitch value R . v_{CN} is the number of course in a 25mm height for the new stitch value, and v_{CR} is the number of course in a 25mm height for the reference stitch value. Once again, each stitch value was used as a reference value to predict the other stitch value results, showing agreement between theoretical and experimental results (Figure 17). Additional work will be required to determine how to mathematically account for the difference in behavior of the higher stitch density samples.

Vertical Transition Sample Extension

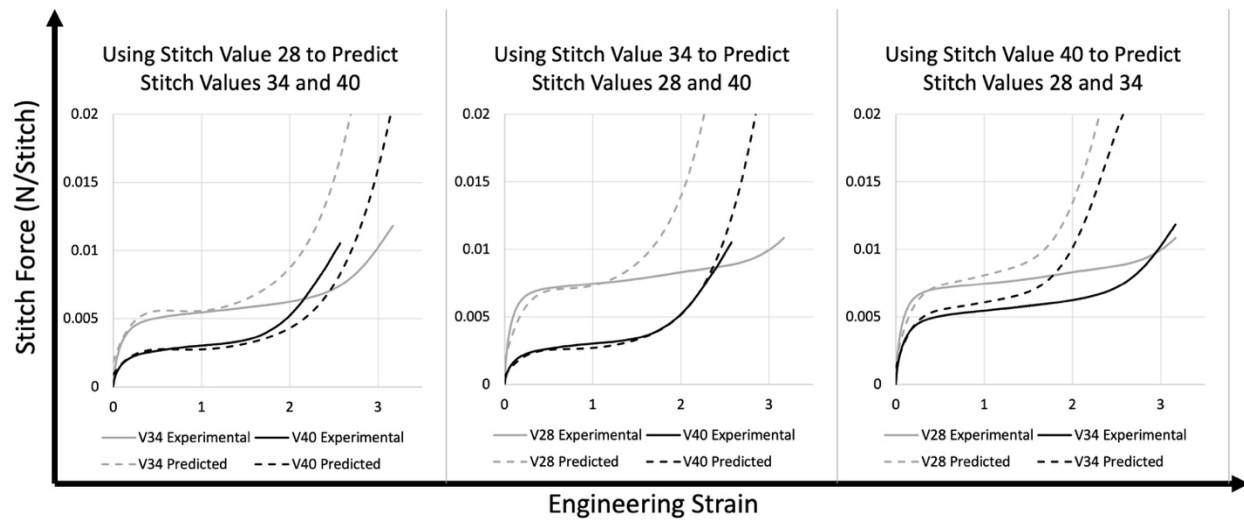


Figure 17. Theoretical prediction of stitch force curves in vertical transition samples

4. Conclusions

In order to predict and control the self-folding behavior of weft knit textiles, a novel system of analyzing the behavior of plain front and back stitch segments has been developed. By understanding that self-folding is a result of interacting edge deformations, the direction of the rolling behavior can be predicted, based on the fabrics tendency to roll towards the front stitch side or back stitch side at a course or wale boundary. The forces driving these rolling behaviors were then quantified, by measuring the interaction between front and back stitch segments that occurred horizontally or vertically across the fabrics. A method was developed to measure and compare the forces driving this behavior in horizontal and vertical transitions between front and back stitches, and how these forces changed with variations in stitch value. It was then demonstrated how this characterization data could be used to begin to control the outcome of self-folding stitch patterns using scaling factors, and furthermore how we can begin to predict this scaling factor mathematically. Future work will further refine the developed equations, to predict the entire data curve as well as to account for fabrics of more extreme density or porosity. While only front and back stitches were studied here, this work lays the foundation for understanding how to study the deformations behaviors of more complex stitch patterns incorporating additional stitches such as tuck, miss. Furthermore, although this study focused on one yarn material, the authors have already begun studying the effects of yarn material changes on self-folding behavior. While yarn material affects the magnitude of the measured data curves, the relationship between horizontal to vertical folding forces remains similar due to the dependance of the folding mechanisms on the knit structure, rather than the yarn structure. By understanding the mechanisms behind self-folding in weft knit fabrics, we have created systems for predicting and controlling this behavior. As we

improve the ability to precisely engineer folding behaviors, we can begin to use these fabric structures for technical applications. It is envisioned that the unique self-folding behaviors can be explored for creation of new types of devices such as textile springs and actuators, deployable fabric architectures, new approaches to composite materials, conformable garments and more.

5. Funding

[Funding info contains potentially identifying information, and therefore has been removed temporarily for the peer review process.]

Declarations of Interests: None

6. Acknowledgements

[Acknowledgments contain identifying information, and therefore have been removed temporarily for the peer review process.]

7. References

1. Zirbel SA, Trease BP, Magleby SP, Howell LL. Deployment Methods for an Origami-Inspired Rigid-Foldable Array. In: *Proceedings of the 40th Aerospace Mechanisms Symposium*. NASA Goddard Space Flight Center, Maryland, USA; 2014.
2. Mulford RB, Jones MR, Iverson BD. Dynamic Control of Radiative Surface Properties With Origami-Inspired Design. *J Heat Transfer*. 2015 Nov 3;138(3):032701-032701-9.
3. Zhai Z, Wang Y, Jiang H. Origami-inspired, on-demand deployable and collapsible mechanical metamaterials with tunable stiffness. *PNAS*. 2018 Feb 27;115(9):2032-7.
4. Knittel CE, Nicholas DS, Street RM, Schauer CL, Dion G. Self-Folding Textiles through Manipulation of Knit Stitch Architecture. *Fibers*. 2015 Dec 15;3(4):575-87.
5. Luan K, West A, DenHartog E, McCord M. Auxetic deformation of the weft-knitted Miura-ori fold. *Text. Res. J*. 2020 Mar 1;90(5-6):617-30.
6. Liu Y, Hu H, Lam JKC, Liu S. Negative Poisson's Ratio Weft-knitted Fabrics. *Text. Res. J*. 2010 Jun 1;80(9):856-63.
7. Glazzard M, Breedon P. Weft-knitted auxetic textile design. *Phys Status Solidi B*. 2014 Feb 1;251(2):267-72.

8. Hu H, Wang Z, Liu S. Development of auxetic fabrics using flat knitting technology. *Text. Res. J.* 2011 Sep 1;81(14):1493–502.
9. Wang Z, Hu H. Auxetic materials and their potential applications in textiles. *Text. Res. J.* 2014 Sep 1;84(15):1600–11.
10. Alderson A, Alderson K. Expanding materials and applications: exploiting auxetic textiles. *Tech Text Int.* 2005;14:29–34.
11. Darja R, Pavko-Čuden A. Foldable weft knitted structures with auxetic potential. In: *International Symposium in Knitting and Apparel - ISKA 2013*. Lasi, Romania; 2013.
12. Steffens F, Rana S, Fanguero R. Development of novel auxetic textile structures using high performance fibres. *Mater. Des.* 2016 Sep 15;106:81–9.
13. Rant D, Ciobanu R, Blaga M, Pavko-Cuden A. Compression of foldable links-links knitted structures. *Tekstil ve Konfeksiyon (Journal of Textile and Apparel)*. 2014;24(4):349–55.
14. Shima Seiki SDS One Apex. Shima Seiki MFG LTD;
15. Peirce FT. 5—the Geometry of Cloth Structure. *J. Text. Inst., Trans.* 1937 Mar 1;28(3):T45–96.
16. Leaf GAV, Anandjiwala RD. A Generalized Model of Plain Woven Fabric. *Text. Res. J.* 1985 Feb 1;55(2):92–9.
17. Hottet GH. An Investigation of Fabric Structure and It's Relation to Certain Physical Properties. *Text. Res. J.* 1950;20(12):811–28.
18. Leaf GAV, Glaskin A. 43—The Geometry of a Plain Knitted Loop. *J. Text. Inst., Trans.* 1955 Sep 1;46(9):T587–605.
19. Choi KF, Lo TY. An Energy Model of Plain Knitted Fabric. *Text. Res. J.* 2003;73(8):739–48.
20. Kurbak A, Ekmen O. Basic Studies for Modeling Complex Weft Knitted Fabric Structures Part I: A Geometrical Model for Widthwise Curlings of Plain Knitted Fabrics. *Text. Res. J.* 2008 Mar 1;78(3):198–208.
21. Kurbak A, Soydan AS. Basic Studies for Modeling Complex Weft Knitted Fabric Structures Part III: A Geometrical Model for 1×1 Purl Fabrics. *Text. Res. J.* 2008 May 1;78(5):377–81.
22. Kurbak A. Geometrical Models for Balanced Rib Knitted Fabrics Part I: Conventionally Knitted 1×1 Rib Fabrics. *Text. Res. J.* 2009 Mar 1;79(5):418–35.
23. Kurbak A. Geometrical models for weft-knitted spacer fabrics
,
Geometrical models for weft-knitted spacer fabrics. *Text. Res. J.* 2017 Mar 1;87(4):409–23.
24. Liu D, Christe D, Shakibajahromi B, Knittel C, Castaneda N, Breen D, et al. On the role of material architecture in the mechanical behavior of knitted textiles. *Int J Solids Struct.* 2017 Mar;109(15):101–11.
25. Liu D, Shakibajahromi B, Dion G, Breen D, Kontsos A. A Computational Approach to Model Interfacial Effects on the Mechanical Behavior of Knitted Textiles. *J Appl Mech.* 2018 Feb 9;85(4):041007-041007–12.
26. Poincloux S, Adda-Bedia M, Lechenault F. Geometry and Elasticity of a Knitted Fabric. *Phys Rev X.* 2018 Jun 22;8(2):021075.
27. Choi, KF, Lo TY. The Shape and Dimensions of Plain Knitted Fabric: A Mechanical Model. *Text. Res. J.* 2006;76(10):777–86.
28. Weeger O, Sakhaei AH, Tan YY, Quek YH, Lee TL, Yueng S-K, et al. Towards a digital workflow for design and fabrication of 3D knitted textiles: nonlinear multi-scale modelling,

simulation and validation. In: *Proceedings of the 8th World Conference on 3D Fabrics and Their Applications*. 2018.

29. Sha S, Ma P, Chapman LP, Jiang G, Zhang A. Three-dimensional modeling and simulation of deformation behavior of fancy weft knitted stitch fabric. *Text. Res. J.* 2017 Sep 1;87(14):1742–51.
30. Guo K, Wang X, Wu Z, Zhang T, Zhou M. Modelling and Simulation of Weft Knitted Fabric Based on Ball B-Spline Curves and Hooke's Law. In: *2015 International Conference on Cyberworlds (CW)*. 2015. p. 86–9.
31. Wu K, Gao X, Ferguson Z, Panozzo D, Yuksel C. Stitch meshing. *ACM Trans Graph.* 2018 Jul 30;37(4):130:1–130:14.
32. Leaf J, Wu R, Schweickart E, James DL, Marschner S. Interactive design of periodic yarn-level cloth patterns. *ACM Trans Graph.* 2018 Dec 4;37(6):202:1–202:15.
33. Kaldor JM, James DL, Marschner S. Simulating knitted cloth at the yarn level. In: *SIGGRAPH '08: Special Interest Group on Computer Graphics and Interactive Techniques Conference*. Los Angeles, CA, USA; 2008. p. 1–9. (SIGGRAPH '08).
34. Yuksel C, Kaldor JM, James DL, Marschner S. Stitch Meshes for Modeling Knitted Clothing with Yarn-level Detail. *ACM Trans Graph.* 2012 Jul;31(4):37:1–37:12.
35. Cirio G, Lopez-Moreno J, Otaduy MA. Yarn-Level Cloth Simulation with Sliding Persistent Contacts. *IEEE Trans Vis Comput Graph* 2017 Feb;23(2):1152–62.
36. Cirio G, Lopez-Moreno J, Otaduy MA. Efficient Simulation of Knitted Cloth Using Persistent Contacts. In: *Proceedings of the 14th ACM SIGGRAPH / Eurographics Symposium on Computer Animation*. Los Angeles, CA, USA: ACM; 2015. p. 55–61. (SCA '15).
37. Chen Y, Lin S, Zhong H, Xu Y-Q, Guo B, Shum H-Y. Realistic Rendering and Animation of Knitwear. *IEEE Trans Vis Comput Graph.* 2003;9(1):43–55.
38. Narayanan V, Albaugh L, Hodgins J, Coros S, McCann J. Automatic Machine Knitting of 3D Meshes. *ACM Trans Graph.* 2018 Aug;37(3):35:1–35:15.
39. Lin J, Narayanan V, McCann J. Efficient Transfer Planning for Flat Knitting. In: *Proceedings of the 2nd ACM Symposium on Computational Fabrication*. Cambridge, Massachusetts: ACM; 2018. p. 1:1–1:7. (SCF '18).
40. Wu K, Swan H, Yuksel C. Knittable Stitch Meshes. *ACM Trans. Graph.* 2019 Jan 19;38(1):1–13.
41. Narayanan V, Wu K, Yuksel C, McCann J. Visual knitting machine programming. *ACM Trans Graph.* 2019 Jul 12;38(4):63:1–63:13.
42. Guest JK, Prévost JH, Belytschko T. Achieving minimum length scale in topology optimization using nodal design variables and projection functions. *Int J Numer Meth Engng.* 2004;61(2):238–54.
43. Oliveira NP, Maciel L, Catarino AP, Rocha AM. Parametric modelling design applied to weft knitted surfaces and its effects in their physical properties. *IOP Conf Ser: Mater Sci Eng.* 2017;254(16):162008.
44. Karmon A, Serman Y, Shaked T, Sheffer E, Nir S. KNITIT: A Computational Tool for Design, Simulation, and Fabrication of Multiple Structured Knits. In: *Proceedings of the 2nd ACM Symposium on Computational Fabrication*. Cambridge, Massachusetts: ACM; 2018. p. 4:1–4:10. (SCF '18).
45. Seyedin S, Razal JM, Innis PC, Wallace GG. A facile approach to spinning multifunctional conductive elastomer fibres with nanocarbon fillers. *Smart Mater. Struct.* 2016 Feb 22;25(3).

Supplemental Data

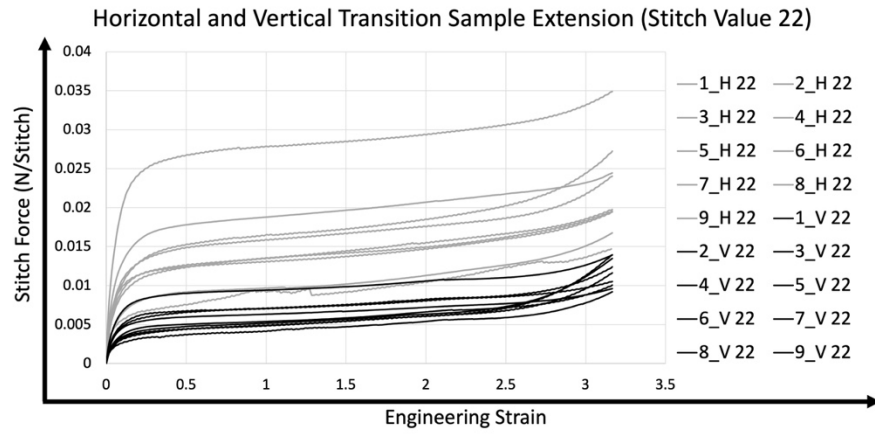


Figure a. Characterization of horizontal and vertical folding samples made at stitch value 22.

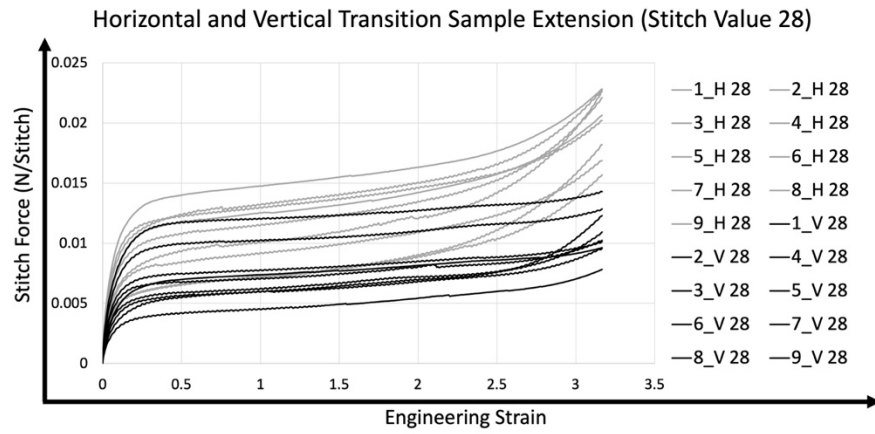


Figure b. Characterization of horizontal and vertical folding samples made at stitch value 28.

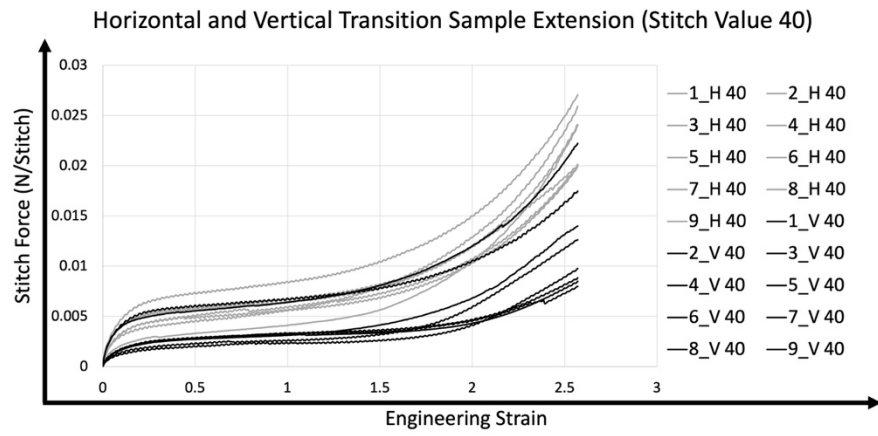


Figure c. Characterization of horizontal and vertical folding samples made at stitch value 40.